JOURNAL OF PHYSICAL ORGANIC CHEMISTRY
J. Phys. Org. Chem. 2000; **13:** 112–126

Conjugated polymers with 2,2′-bipyridine and diethinylenebenzene units: absorption and luminescence properties

U.-W. Grummt,[1]* E. Birckner,[1] E. Klemm,[2] D. A. M. Egbe[2] and B. Heise[2]

[1]Institut für Physikalische Chemie der Friedrich-Schiller Universität Jena, Lessingstrasse 10, D-07743 Jena, Germany
[2]Institut für Organische und Makromolekulare Chemie der Friedrich-Schiller Universität Jena, Humboldtstrasse 10, D-07749 Jena, Germany

Received 22 June 1999; revised 4 October 1999; accepted 8 October 1999

ABSTRACT: Alternating oligomers and polymers consisting of 2,2′-bipyridine and diethinylenebenzene units and corresponding model compounds were synthesized and investigated in dilute solutions by absorption spectroscopy and by stationary and time-resolved emission spectroscopy. The strictly linear (rod-like) π-chain oligomers/polymers were compared with the angularly linked oligomers/polymers and with related model compounds. The model compounds which already show the essential spectroscopic properties of the oligomers/polymers consist of three (hetero)aromatics linearly connected by two diethenylene groups. These models exhibit fluorescence quantum yields close to unity and short fluorescence decay times around 1 ns. Fluorescence anisotropy and rotational relaxation times are consistent with the Stokes–Einstein equation and the Perrin equation. The absorption and emission spectra of the polymers and their radiative rate constants determined by fluorescence quantum yield and lifetime and according to the Strickler/Berg equation show a conjugation length of one to two repetition units. The conjugation along the chain is stronger in linear than in angular polymers and stronger in alkoxy-substituted than in unsubstituted polymers. In angular polymers at least two different emitting segments were found. The shortened mean lifetimes and the reduced fluorescence quantum yields and anisotropies of the oligomers/polymers indicate an additional radiationless deactivation channel which is opened by energy migration along the chain. Rates of energy transfer calculated for linear and angular polymers correlate with rates of radiationless deactivation.

KEYWORDS: 2,2′-bipyridine; diethinylenebenzene; conjugated polymers; absorption; luminescence

INTRODUCTION

Highly fluorescent conjugated polyarenes have been of increasing interest as potential materials for electroluminescence devices and attract particular attention because of their high non-linear susceptibilities,[1,2] which make them candidates for all optical switching devices.[3]

From the point of view of more fundamental research, segmented conjugated polyarenes are useful objects for investigating energy migration along the polymer chain.[4] In particular, fluorescent rigid rod oligomers including suitable model compounds are excellent probes for studying molecular motions in viscous media by static and kinetic monitoring of the fluorescence anisotropy. An additional interesting aspect is their potential use as molecular wires.[5]

Several papers have been appeared in recent years which deal with the synthesis and spectroscopic characterization of poly(phenyleneethinylenes) and alternating poly(phenyleneethinylen/heteroarylethinylenes). Among others, stilbene-4,4′-diyl, anthracene-9,10-diyl, thiene-2,5-diyl and pyridine-2,5-diyl have been used as arylenes and heteroarylenes. In order to increase the solubility of these rigid, linear polymers, alkyl side-chains have been introduced via ester, ether or other groups. Kondo *et al.* reported on a poly(phenyleneethinylene) which is well soluble due to its angular structure.[6]

Essentially, absorption and fluorescence spectra have been published, and sometimes also fluorescence quantum yields. From a comparison of absorption spectra with fluorescence excitation spectra, Morgan *et al.*[7] concluded that energy transfer occurs along the polymer chain. Efficient energy transfer has been found by Swager[8] with anthracene terminal groups. This group exploits energy transfer to enhance significantly the sensitivity of a fluorescent chemosensor.[9] Picosecond time-resolved measurements and investigations into the stimulated emission have been published.[10,11] Ley and co-workers published the synthesis and photophysical data for two

**Correspondence to:* U.-W. Grummt, Institut für Physikalische Chemie der Friedrich-Schiller Universität Jena, Lessingstrasse 10, D-07743 Jena, Germany.
E-mail: cug@rz.uni-jena.de

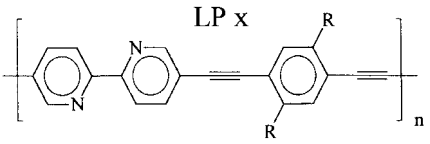

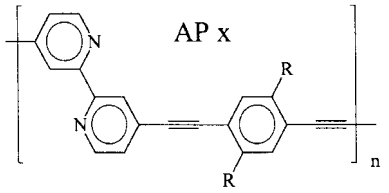

Code	R	DP
LP1	H	≤ 4
LP2	OC_8H_{17}	10
LP3	OC_8H_{17}	13
LP4	$OC_{18}H_{37}$	6
LP5	$OC_{18}H_{37}$	11
LP6	$OC_{18}H_{37}$	19

Code	R	DP
AP1	H	≤ 4
AP2	$OC_{12}H_{25}$	19
AP3	$OC_{18}H_{37}$	10
AP4	$OC_{18}H_{37}$	25

Scheme 1

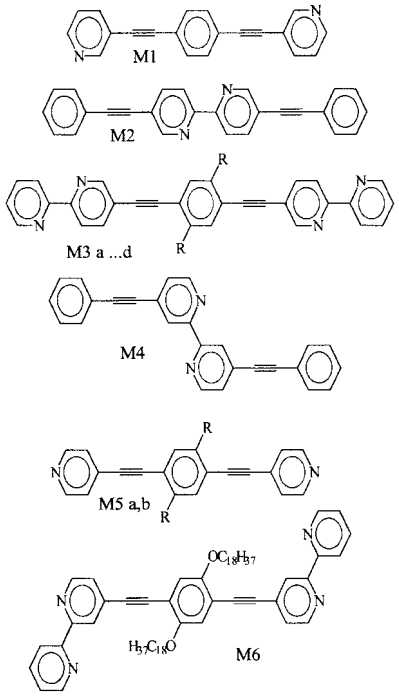

Code	R
M3a	H
M3b	OC_8H_{17}
M3c	$OC_{12}H_{25}$
M3d	$OC_{18}H_{37}$

Code	R
M5a	H
M5b	OC_8H_{17}

Scheme 2

model compounds and one polymer containing 2,2′-bipyridyl in the backbone including their metal complexes.[12] Systematic investigations into the photophysics have been published for only two compounds.[11]

In this paper, we report on absorption and emission of new linear and angular conjugated polymers, oligomers and their model compounds consisting of 2,2′-bipyridine and diethinylenebenzene units in the backbone. It was the aim of this study to identify the chromophore unit and to unravel the effect of structural variation, particularly the comparison of a linear or angular backbone, on the photophysical deactivation and energy transfer along the chain.

The conjugated alternating oligomers and polymers investigated contain 2,2′-bipyridine and 1,4-substituted diethinylenebenzene as building blocks. As shown in Scheme 1, two different types of linkage are realized.

The abbreviations **L** and **A** stand for the linear and angular linkage, respectively, and **P** and **M** designate polymers (or oligomers) and model compounds, respectively. Owing to the synthetic route the terminating atoms are bromine. Acetylene moieties as terminating groups could be excluded by NMR spectroscopy.

In order to determine the chromophore unit and to understand the photophysical behaviour of the oligomers and the polymers, we compared them with their related model compounds. Owing to the spectral location of the long-wavelength absorption band and particularly the high fluorescence quantum yield, compounds with at least three aryl units connected by two acetylene groups should be considered as models.

The model compounds and their abbreviations are given in Scheme 2.

The polymers and the higher oligomers without alkoxy substituents are insoluble. Therefore, only oligomers with chain lengths up to a mean degree of polymerization (DP) of 4 could be investigated. Alkoxy substitution increases the solubility of the compounds and opens the possibility of investigating higher oligomers and polymers.

EXPERIMENTAL

Synthesis

The syntheses of several compounds investigated in this work have been published previously.[13] All chemicals were purchased from Fluka and Aldrich. Toluene was dried and distilled over calcium hydride and, THF, triethylamine and diisopropylamine were distilled over potassium hydroxide. All solvents were degassed by

bubbling with argon for 1 h prior to use. All reactions were carried out under an inert gas atmosphere (argon).

Synthesis of reactands

1,4-Diethinylbenzene[14] and 2,5-di(octyloxy)-, 2,5-di(dodecyloxy) and 2,5-di(octadecylyloxy)-1,4-diethinylbenzene[8,15,16] were prepared by published procedures. The syntheses of 5-bromo- and 5,5′-dibromo-2,2′-bipyridine were performed according to Romero and Ziessel.[17] 4-Bromo- and 4,4′-dibromo-2,2′-bipyridine were synthesized as described.[18,19]

Synthesis of the model compounds

1,4-Bis(3′-pyridylethinyl)benzene (M1). Tetrakis(triphenylphosphine)palladium [$Pd(PPh_3)_4$] (48 mg, 0.09 mmol, 2.3 mol%) and copper(I) iodide (CuI) (16 mg, 0.08 mmol, 2.0 mol%) were added to a degassed solution of 1,4-diethinylbenzene (0.5 g, 4 mmol) and 3-bromopyridine (1 ml, 10 mmol) in triethylamine (3 ml) and toluene (40 ml). The reaction mixture was stirred and heated under reflux for 7.5 h, then filtered hot to remove the inorganic compounds. After cooling to room temperature a dark-red solid precipitated. The resulting suspension was poured into an excess of methanol and the dark-red precipate collected by filtration. 1,4-Bis(3′-pyridylethinyl)benzene was isolated from the filtrate. The solvent was removed under vacuum and the residue purified by column chromatography on silica gel 60. The starting materials 1,4-diethinylbenzene and 3-bromopyridine were reisolated by elution with toluene–ethyl acetate (1:1, v/v). Byproducts of higher molecular weight were removed again by column chromatography (silica gel 60) with toluene–ethyl acetate as eluent (gradient elution, 9:1–1:9, v/v). Final purification by vacuum sublimation (135 °C, 3×10^{-2} mbar) yielded a white powder; yield 30 mg (3%), m.p. 175–177 °C.

^{1}H NMR ($CDCl_3$): δ = 7.28 (2 H, q, $H_{5'}$), 7.53 (4 H, s, H_{Phe}), 7.78 (2 H, dt, $H_{6'}$), 8.54 (2 H, dd, $H_{2'}$), 8.76 (2 H, d, $H_{4'}$) ppm. ^{13}C NMR ($CDCl_3$): δ = 88.02 (—C≡C—), 92.12 (—C≡C—), 120.16 ($C_{3'}$), 122.91 (C_{Phe}—≡—), 123.08 ($C_{5'}$), 131.69 (C_{Phe}—H), 138.43 ($C_{6'}$), 148.82 ($C_{2'}$), 152.28 ($C_{4'}$) ppm. MS (EI): calculated *m*/*z* = 280 (M), found *m*/*z* = 280 $(M)^+$, 174 $(M - {\equiv} - Ph)^+$, 140 (1/2 $M)^+$, 126 $({\equiv} - Ph - {\equiv})^+$ g mol^{-1}. IR (KBr): ν = 3070 and 3034 (w, C_{aryl}—H), 2225 (m, —C≡C—), 1579 and 1543 (m, —C = N—, —C = C—) cm^{-1}. UV/VIS (1,4-dioxane): λ_{max} (logε) = 319 (4.69), 338 (4.53) nm (ε in l mol^{-1}cm^{-1}). Analysis: $C_{20}H_{12}N_2$ (280.33) calculated C 85.71, H 4.29, N 10.00; found C 84.81, H 4.59, N 9.39%.

M3 compounds. 1,4-Bis(2′,2″-bipyridine-5″-ylethinyl)-benzene (**M3a**) was prepared according to El-Ghayoury and Ziessel.[20] 1,4-Bis(2′,2″-bipyridine-5″-ylethinyl)-2,5-di(octyloxy)benzene (**M3b**) and 1,4-bis(2′,2″-bipyridine-5″-ylethinyl)-2,5-di(dodecyloxy)benzene (**M3c**) were prepared similarly to 1,4-bis(2′,2″-bipyridine-5″-ylethinyl)-2,5-di(octadecyloxy)benzene (**M3d**).[13]

M3b was purified by column chromatography on silica gel 60 eluting with *n*-hexane–THF (2:1, v/v); yield 70%, m.p. 113–115 °C.

^{1}H NMR ($CDCl_3$): δ = 0.83 (6 H, t, —CH_3), 1.25–1.91 [24 H, m, —$(CH_2)_6$—], 4.04 (4 H, t, —CH_2O—), 7.04 (2 H, s, H_{Phe}), 7.30 (2 H, t, $H_{5''}$), 7.80 (2 H, t, $H_{4''}$), 7.90 (2 H, dd, $H_{4'}$), 8.40 (4 H, d, $H_{3'}$ and $H_{3''}$), 8.67 (2 H, d, $H_{6''}$), 8.80 (2 H, d, $H_{6'}$) ppm. ^{13}C NMR ($CDCl_3$): δ = 14.05(CH_3—), 22.63, 26.05, 29.29, 29.33, 29.67, 31.79 [—$(CH_2)_6$—], 69.66 (—CH_2O—), 90.07 and 92.03 (—C≡C—), 113.87 (C_{Phe}—C≡C—), 116.84 (C_{Phe}—H), 120.32 ($C_{5''}$), 120.44 ($C_{5'}$), 121.32 ($C_{3''}$), 123.87 ($C_{3'}$), 136.91 ($C_{4''}$), 139.19 ($C_{4'}$), 149.27 ($C_{6''}$), 151.61 ($C_{6'}$), 153.78 (C_{Phe}—OR), 154.83 ($C_{2''}$), 155.49 ($C_{2'}$) ppm. MS (CI): calculated *m*/*z* = 690 (M), found *m*/*z* = 691 $(M + 1)^+$, 579 $(M - C_8H_{17} + 1)^-$, 466 $(M - 2\ C_8H_{17} + 1)^+$ g mol^{-1}. IR (KBr): ν = 3049 (w, C_{aryl}—H), 2923 and 2854 (vs, CH_2— and CH_3—), 2208 (w, disubstituted —C≡C—), 1390 (m, CH_3—), 1275 (m, aryl— OR) cm^{-1}. UV/VIS ($CHCl_3$): λ_{max}(logε) = 330 (4.67), 387 (4.69) nm. Analysis: $C_{46}H_{50}N_4O_2$ (690.93), calculated C 79.97, H 7.29, N 8.11; found C 79.83, H 7.59, N 7.94%.

M3c was purified by column chromatography on silica gel 60 eluting with *n*-hexane–THF 2:1, (v/v), yield 60%, m.p. 100–102 °C.

^{1}H NMR ($CDCl_3$): δ = 0.83 (6 H, t, —CH_3), 1.21–1.91 [40 H, m, —$(CH_2)_{10}$—], 4.04 (4 H, t, —CH_2O—), 7.04 (2 H, s, H_{Phe}), 7.30 (2 H, ddd, $H_{5''}$), 7.81 (2 H, ddd, $H_{4''}$), 7.90 (2 H, dd, $H_{4'}$), 8.40 (4 H, d, $H_{3'}$ and $H_{3''}$), 8.67 (2 H, d, $H_{6''}$), 8.80 (2 H, d, $H_{6'}$) ppm. ^{13}C NMR ($CDCl_3$): δ = 13.99 (CH_3—), 22.57, 25.98, 29.25, 29.30, 29.54, 29.57, 31.80 [—$(CH_2)_{10}$—], 69.59 (—CH_2O—), 91.04 (—C≡C—), 113.80 (C_{Phe}—*C*≡C—), 116.76 (C_{Phe}—H), 120.25 ($C_{5''}$), 120.38 ($C_{5'}$), 121.20 ($C_{3''}$), 123.82 ($C_{3'}$), 136.85 ($C_{4''}$), 139.15 ($C_{4'}$), 149.20 ($C_{6''}$), 151.54 ($C_{6'}$), 153.71 (C_{Phe}-OR), 154.74 ($C_{2''}$), 155.39 ($C_{2'}$) ppm. MS (CI): calculated *m*/*z* = 802 (M), found *m*/*z* = 803 $(M + 1)^+$, 635 $(M - C_{12}H_{25} + 1)^+$, 466 $(M - 2C_{12}H_{25} + 1)^+$, 401 g mol^{-1}. IR (KBr): ν = 3056 (w, C_{aryl}— H), 2922 and 2851 (vs, CH_2— and CH_3—), 2207 (w, disubstituted —C≡C—), 1389 (m, CH_3—), 1274 (m, C_{aryl}— OR) cm^{-1}. UV/VIS ($CHCl_3$): λ_{max} (logε) = 330 (4.67), 388 (4.67) nm. Analysis: $C_{54}H_{66}N_4O_2$ (803.14) calculated C 80.75, H 8.28, N 6.97; found C 80.20, H 8.40, N 6.73%.

4,4′-Bis(phenylethinylene)-2,2′-bipyridine (M4). $Pd(PPh_3)_4$ (9 mg, 0.00075 mmol, 1.0 mol%) and CuI (3 mg, 0.0015 mmol, 2.1 mol%) were added to a mixture of 4,4′-dibromo-2,2′-bipyridine (230 mg, 0.73 mmol), phenylacetylene (154 mg, 1.47 mmol) and triethylamine (1 ml) in dried toluene (10 ml). The reaction mixture was

stirred at reflux for 3 h, then poured into methanol (200 ml). The precipitate was purified by column chromatography with *n*-hexane–THF (3:1, v/v). A 150 mg amount of white crystals was obtained, yield 57.4%, m.p. 203–205 °C.

^{1}H NMR ($CDCl_3$): δ = 7.36–7.41 (8 H, m, H_{Phe}), 7.53–7.57 (4 H, m, H_{Phe} and H_3), 8.52 (2 H, s, H_5), 8.66 (2 H, d, H_6) ppm. ^{13}C NMR ($CDCl_3$): δ = 86.98 (—C≡C—), 94.08 (—C≡C—), 122.24 (C_{Phe}—≡—), 123.27 (C_{Phe}), 125.51 (C_{Phe}), 128.49 (C_{Phe}), 129.16 (C_3), 131.93 (C_5), 132.58 (C_4), 149.23 (C_6), 155.69 (C_2) ppm. MS (CI): calculated m/z = 356 (M), found m/z = 357 $(M + 1)^+$, 178(1/2 M)$^+$ g mol^{-1} IR (KBr): ν = 2216 (m, disubstituted —C≡C—) cm^{-1}. UV/VIS ($CHCl_3$): λ_{max} (logε) = 268 (4.59), 291 (4.70), 306 (4.71) nm. Analysis: $C_{26}H_{16}N_2$ (356.41) calculated C 87.62, H 4.52, N 7.86; found C 87.17, H 4.67, N 7.85%.

1,4-Bis(4′-pyridylethinyl)benzene (M5a). 4-Bromopyridine was prepared from 4-bromopyridine hydrochloride (3 g, 19 mmol) by treatment with 4 N aqueous sodium hydroxide (10 ml). The resulting emulsion was extracted twice with diethyl ether, the ether solutions were dried over magnesium sulphate and the solvent was removed immediately before use.

M5a was prepared and purified analogously to **M1**, replacing the 3-bromopyridine by 4-bromopyridine (2 g, 12 mmol). Vacuum sublimation (150 °C, 4×10^{-3} mbar) yielded a white substance, yield 150 mg (13%), m.p. 169–171 °C.

^{1}H NMR ($CDCl_3$): δ = 7.36 (4 H, dd, $H_{2'}$), 7.54 (4 H, s, H_{Phe}), 8.60 (4 H, dd, $H_{3'}$) ppm. ^{13}C NMR ($CDCl_3$): δ = 88.80 (—C≡C—), 93.15 (—C≡C—), 122.87 ($C_{1'}$), 125.48 ($C_{2'}$), 131.01 (C_{Phe}), 131.91 (C_{Phe}), 149.85 ($C_{3'}$) ppm. MS (EI): calculated m/z = 280 (M), found m/z = 280 (M)$^+$, 174 (M −≡—Ph)$^+$, 140 (1/2 M$^+$, 126 (≡—Ph—≡)$^+$ g mol^{-1}. IR (KBr): ν = 3075 and 3039 (w, C_{aryl}−H), 2222 (m, —C≡C—), 1587 and 1538 (m, —C=C—, —C=N) cm^{-1}. UV/VIS (1,4-dioxane): λ_{max} (logε) = 318 (4.61), 336 (4.52) nm. Analysis: $C_{20}H_{12}N_2$ (280.33): calculated C 85.71, H 4.29, N 10.00; found C 85.35, H 4.77, N 9.54%.

The synthesis of **M5a** and metal complexes therefrom has already been reported.[21] **M5a** was described as a yellow–orange powder, which leads us to the suspicion that the product contained impurities with diacetylene substructures which are generated by oxidative coupling reactions.

2,5-Bis(octyloxy)-1,4-di(4′-pyridylethinyl)benzene (M5b). 4-Bromopyridine was liberated from 4-bromopyridine hydrochloride as described before. 4-Bromopyridine (0.5 g, 3 mmol) and 2,5-di(octyloxy)-1,4-diethinylbenzene (0.4 g, 1 mmol) were dissolved in degassed diisopropylamine (2 ml) and toluene (10 ml). Tetrakis(triphenylphosphine)palladium (12 mg, 0.02 mmol) and copper(I) iodide (4 mg, 0.02 mmol) were added and the reaction mixture was stirred for 1 h at room temperature and afterwards heated for 3 h under reflux. After cooling to room temperature, the reaction mixture was poured into an excess of methanol and the resulting brownish precipate and inorganic compounds were collected by filtration. 2,5-Di(octyloxy)-1,4-bis(4′-pyridylethinyl)benzene was isolated from the filtrate, which was concentrated under reduced pressure.

The starting products 4-bromopyridine and 2,5-di(octyloxy)-1,4-diethinylbenzene were removed by column chromatography (silica gel 60) with hexane–ethyl acetate (1:1, v/v) as eluent. Further fractionation of the residue by column chromatography on alkaline aluminium oxide eluting with hexane–ethyl acetate (gradient elution, 9:1–1:9, v/v) afforded a fraction of pure 2,5-di(octyloxy)-1,4-bis(4′-pyridylethinyl)benzene (20 mg, yield 0.9%) and fractions containing mixtures of 2,5-di(octyloxy)-1,4-bis(4′-pyridylethinyl)benzene and side-product 1,4-bis [2′,5′-dioctyloxy-1′-4″-pyridylethinyl)-benzyl]butadiyne (altogether 300 mg, yield 13.9%).

^{1}H NMR ($CDCl_3$): δ = 0.85 (6 H, t, —CH_3), 1.53–1.23 [20 H, m, —$(CH_2)_5$—], 1.83 (4 H, m, —OCH_2CH_2—), 4.01 (4 H, t, —OCH_2—), 7.01 (2 H, s, H_{Phe}), 7.35 (4 H, d, H_2), 8.59 (4 H, d, H_3) ppm. ^{13}C NMR ($CDCl_3$): δ = 14.07 (—CH_3), 22.56, 26.05, 29.24, 29.30, 29.68 [—$(CH_2)_5$—], 31.78 (—OCH_2CH_2—), 69.56 (OCH_2—), 90.32 (—C≡C—), 92.29 (—C≡C—), 113.68 (C_{Phe}—≡—), 116.85 (C_{Phe}), 125.40 ($C_{2'}$), 131.42 ($C_{1'}$), 149.77 ($C_{3'}$), 153.87 (C_{Phe}-OR) ppm. MS (CI): calculated m/z = 536 (M), found m/z = 537 $(M + H)^+$, 425 $(M + H - C_8H_{17})^+$, 312 $(M + H - 2\ C_8H_{17})^+$ g mol^{-1}. UV/VIS (1,4-dioxane): λ_{max} (logε) = 237 (4.34), 307 (4.49), 316 (sh, 4.44), 373 (4.36) nm. Analysis: $C_{36}H_{44}N_2O_2$ (536.76) calculated C 80.60, H 8.21, N 5.22; found C 80.09, H 8.46, N 5.66%.

1,4- Bis(2′,2″-bipyridine-4″-ylethinyl)-2,5-di(octadecyloxy)benzene (M6). 4-Bromo-2,2′-bipyridine (640 mg, 2.72 mmol), 1,4-diethynyl-2,5-di(octadecyloxy)benzene (862 mg, 1.3 mmol), $Pd(PPh_3)_4$ (63 mg, 0.053 mmol, 2 mol%) and CuI (12 mg, 0.053 mmol) were dissolved to a degassed solution of diisopropylamine (15 ml) and THF (60 ml) under an Ar atmosphere. The mixture was heated at reflux for 24 h. After cooling to room temperature, it was added dropwise to 400 ml of vigorously stirred methanol. After stirring for 15 min, the precipitate was collected by filtration, dissolved in THF (40 ml), passed through a 3 ml plug of silica gel and then poured once more into methanol. The collected solid was purified through column chromatography on silica gel eluting with *n*-hexane–THF (2:1, v/v) and by reprecipitation of its THF solution into methanol. A bright yellow solid was obtained, yield 1.14g (90%), m.p. 104–106 °C. ^{1}H NMR ($CDCl_3$): δ = 0.85 (6 H, t, —CH_3), 1.19–1.86 [64 H, m, —$(CH_2)_{16}$—], 4.04 (4 H, t, —CH_2O—), 7.03 (2 H, s, H_{Phe}), 7.31 (2 H, t, $H_{5''}$), 7.37 (2 H, dd, $H_{5'}$), 7.81 (2 H, ddd, $H_{4''}$), 8.38 (2 H, d, $H_{3''}$), 8.52 (2 H, s, $H_{3'}$), 8.64 (2

Table 1. Mean degree of polymerization (DP), number- and weight-average molecular weights ($\overline{M}_n$, $\overline{M}_w$) and polydispersity index ($\overline{M}_w/\overline{M}_n$) of polymers obtained from samples prepared with various reaction times

Code	R	DP	Reaction time (h)	$\overline{M}_n$(g mol^{-1})	$\overline{M}_w$(g mol^{-1})	$\frac{\overline{M}_w}{\overline{M}_n}$
LP1	H	≤4	3	1250[a]	—	—
LP2	C_8H_{17}	10	48	5332	13130	2.46
LP3	C_8H_{17}	13	48	6907	13460	1.95
LP4	$C_{18}H_{37}$	6	24	4660	23800	5.11
LP5	$C_{18}H_{37}$	11	24	8541	23350	2.70
LP6	$C_{18}H_{37}$	19	48	15260	30160	1.97
AP1	H	≤4	5	1362[a]	—	—
AP2	$C_{12}H_{25}$	19	48	12310	31750	2.57
AP3	$C_{18}H_{37}$	10	24	8181	11940	1.45
AP4	$C_{18}H_{37}$	25	48	29790	50570	2.80

[a] Elemental analysis, calculated with two bromo endgroups.

H, d, $H_{6''}$), 8.67 (2 H, $H_{6'}$) ppm. ^{13}C NMR ($CDCl_3$): 14,09 (CH_3—), 22.67, 26.09, 29.28, 29.35, 29.41, 29.68, 31.91 [—$(CH_2)_{16}$—], 69.72 (—CH_2O—), 90.43 and 92.67 (—C≡C—), 113.90 (C_{Phe}—C≡C—), 117.19 (C_{Phe}—H), 121.14 ($C_{3''}$), 123.11 ($C_{3'}$), 123.94 ($C_{5''}$), 125.18 ($C_{5'}$), 132.48 ($C_{4''}$), 136.93 ($C_{4'}$), 149.13 ($C_{6''}$), 149.22 ($C_{6'}$), 153.89 (C_{Phe}-OR), 155.61 ($C_{2''}$), 156.28 ($C_{2'}$) ppm. MS (CI): calculated $m/z = 971$ (M), found. $m/z = 972$ $(M + 1)^+$, 719 $(M - C_{18}H_{37})^+$, 485 (1/2 M)$^+$, 465(M $-2\ C_{18}H_{37})^+$, 87 g mol^{-1}. IR (KBr): $\nu = 3055$ (w, C_{aryl}—H), 2918 and 2850 (vs, CH_2— and CH_3—), 2214 (s, disubstituted —C≡C—), 1394 (m, CH_3—), 1279 (m, C_{Aryl}—OR) cm^{-1}. UV/VIS ($CHCl_3$): λ_{max} (logε) = 286 (4.46), 310 (4.46), 380 (4.48) nm. UV/VIS (1,4-dioxane): λ_{max} (logε) = 285 (4.59), 310 (4.57), 319 (4.52), 379 (4.49) nm. Analysis: $C_{66}H_{90}N_4O_2$ (971.46) calculated C 81.60, H 9.33, N 5.76; found C 81.40, H 9.62, N 5.66%.

Polycondensation

Poly[5,5′-(1″,4″-diethinylene-phenylene)-2,2′bipyridylene] (LP1). 1,4-Diethinylbenzene (350 mg, 2.78 mmol), 5,5′-dibromo-2,2′-bipyridine (872 mg, 2.78 mmol), $Pd(PPh_3)_4$ (34 mg, 0.029 mmol, 1.0 mol%) and CuI (13 mg, 0.065 mmol, 2.3 mol%) were added to a degassed solution of triethylamine (3 ml) and toluene (75 ml). After stirring the reaction mixture under reflux for 3 h, it was poured into an excess amount of methanol. The precipitate was collected by filtration and washed repeatedly with methanol. The resulting yellow solid was extracted with hot toluene using a Soxhlet extractor to separate the toluene-soluble fraction, which was used for the spectroscopic investigations. The insoluble part was dried in vacuum. Yield 0.70 g (90.6%), M_n = 1250 g mol^{-1}.

IR (KBr): $\nu = 3293$ (w, ≡C—H), 2216 (w, —C≡C—), 2105(vw, —C≡C—H), 1700 (m, —C=N—), 836 (vs, *p*-disubstituted benzene) cm^{-1}. Analysis: $(C_{20}H_{10}N_2)_n$ $(278.31)_n$ calculated C 86.31, H 3.62, N 10.06; found C 74.34, H 3.55, N 8.15, Br 12.08%.

The preparation procedures of the other polymers have been published previously.[13] In this work some polymers of the same type were investigated which vary in the chain length.

Mean degree of polymerization. The mean degrees of polymerization (DP) for the polymers **LPx** and **APx** (Scheme 1) were calculated from the average molecular weights M_n. The molecular weights of the soluble polymers were determined by gel permeation chromatography in THF, using a UV detector, and an RI detector, and were calibrated with respect to polystyrene standards. The alkoxy-substituted polymers are completely soluble in usual organic solvents. The number-average molecular weights of the poorly soluble polymers **LP1** and **AP1** were estimated through the bromine content from the elemental analysis with the assumption that bromine is at either end of the polymers. These values are approximate ones; small contents of acetylene end-groups were observed for both poorly soluble polymers by IR spectroscopy. For the soluble polymers acetylene end-groups were excluded by NMR spectroscopy.

Mean degrees of polymerization (DP), mean molecular weights ($\overline{M}_n$, $\overline{M}_w$) and polydispersity indices (M_w/M_n) are given in Table 1.

Apparatus, spectroscopic procedures and data evaluation

Melting-points were measured on a Büchi 530 melting apparatus. Mass spectrometry was performed using chemical ionization with H_2O vapour as gas on a Finnigat Mat SSQ 710 instrument. ^{1}H and ^{13}C NMR spectra were taken on a Bruker DRX 400 and a Bruker AC 250 spectrometer, respectively. Gel permeation chromatographic molecular weight determinations were made at a flow-rate of 1 ml min^{-1} in THF on Jasco UV 975 and RI 930 instruments with SDV columns with 10^3, 10^4 and 10^6 Å pore sizes and with polystyrene as standard. The ε values were determined in $CHCl_3$ and/or 1,4-dioxane (for

Table 2. Absorption maxima (λ_a) molar absorptivities (ϵ), fluorescence maxima (λ_f), quantum yields (Φ_f) and lifetimes (τ) or mean lifetimes ($<\tau>$) of (a) model compounds and (b) linear and angular polymers in toluene at room temperature

(a)

Code	R	λ_a (nm)	ε[b] (l mol^{-1} cm^{-1})	λ_f (nm)	Φ_f[c]	τ[c] (ns)
BPB[a]	—	322	62000	349	0.79	0.68
M1	—	322	48900	349	0.83	0.67
M2	—	343	58000	377	0.95	0.69
M3a	—	351	49400	381	0.76	0.55
M3b	OC_8H_{17}	389	49000	430	0.94	1.15
M3c	$OC_{12}H_{25}$	388	47000	430	0.89	1.20
M3d	$OC_{18}H_{37}$	390	48000	431	1	1.12
M4	—	305	52000	345	0.05	<0.02
M5a	—	318	40700[d]	348	0.49	0.51
M5b	OC_8H_{17}	373	25000	419	0.87	2.39
M6	$OC_{18}H_{37}$	381	30400	424	0.90	2.22

(b)

Code	R	DP[e]	λ_a (nm)	ε[f] (l mol^{-1} cm^{-1})	λ_f (nm)	Φ_f[g]	$<\tau>$[g] (ns)
LP1	H	≤4	357	—	388	0.61	0.38
LP2	OC_8H_{17}	10	413	(24200)	454	0.62	0.70
LP3	OC_8H_{17}	13	413	33000	456	0.67	0.65
LP4	$OC_{18}H_{37}$	6	406	30000	452	0.55	0.70
LP5	$OC_{18}H_{37}$	11	420	41000	454	0.48	0.75
LP6	$OC_{18}H_{37}$	19	421	40000	456	0.45	0.55
AP1	H	≤4	329	20900	389	0.45	0.42
AP2	$OC_{12}H_{25}$	19	387	25000	446	0.57	0.9
AP4	$OC_{18}H_{37}$	25	386	29000	445	0.62	1.18

[a] **BPB** = 1,4-bisphenylethinylbenzene.
[b] Solvent chloroform, ±10%.
[c] ±10%.
[d] In dioxane.
[e] Mean degree of polymerization,
[f] Per mole of repeating unit, solvent chloroform.
[g] ±20%.

HPLC, Baker) on a Perkin-Elmer Lambda 19 UV/VIS–NIR spectrometer. A Nicolet Impact 400 spectrometer was used for IR measurements. Elemental analysis was performed on a Leco CHNS-932 Automat.

The solvents toluene and ethanol used for the spectroscopic investigations were of spectroscopic grade (Uvasol, Merck). The fluorescence of fluid paraffin oil (Merck) used for polarization measurements was less than 1% of the fluorescence of the investigated model compounds or polymers under the same experimental conditions.

Absorption spectra at room temperature and at low temperatures were recorded on a Lambda 16 spectrophotometer (Perkin-Elmer) equipped with an NKT Kryostat. PMMA cells were used for low-temperature absorption measurements (near 77 K). Mostly, the optical quality of the low-temperature glasses is better in PMMA cells than in quartz cells, probably owing to the greater flexibility of PMMA.

Fluorescence and phosphorescence emission and excitation spectra and steady-state fluorescence polarization spectra were measured with an LS50B luminescence spectrometer (Perkin-Elmer).

Fluorescence quantum yields were calculated relative to quinine sulphate (purum, Fluka) in 0.1 N H_2SO_4 (pro analysi, Laborchemie Apolda) used as a standard ($\Phi_f = 0.55$) according to Ref. 22. The absorbance at the excitation wavelength was kept below 0.05 for the samples and the reference.

Fluorescence kinetics were investigated with a CD900 time correlating single photon counting spectrometer (Edinburgh Instruments). The excitation source was a hydrogen-filled nanosecond flashlamp giving an instrument response pulse of 1.3 ns FWHM. Polarizers with a vertical orientation on the excitation side and a 55° (magic angle) orientation on the emission side were used to avoid polarization effects. Decay curves were accumulated until 10^4 counts in the maximum with at least 10^3 occupied channels. In order to determine rotational relaxation times directly from kinetic measurements, the decay curves were measured with a parallel and a perpendicular oriented analyzer. These measurements were performed with the highest possible time resolution of the multi-channel analyzer (6 ps per channel).

To calculate the fluorescence lifetime and the rota-

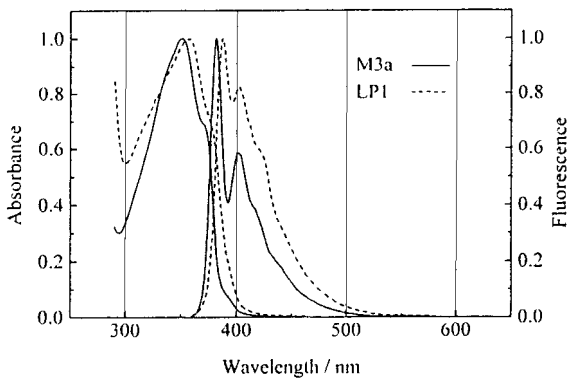

Figure 1. Absorption and fluorescence spectra of the unsubstituted oligomer **LP1** (dashed line) and the related model **M3a** (solid line) in toluene at room temperature

tional relaxation time from the decay curves, the Level 1 (up to four exponentials) and Level 2 (spherical rotor anisotropy) packages implemented in the Edinburgh Instruments software were used. (The analysis makes use of the iterative reconvolution technique and the Marquardt fiiting algorithm.) Plots of weighted residuals and of the autocorrelation function and values of reduced residuals χ^2 were used to judge the quality of the fit. Values of χ^2 larger than 1.3 were not accepted. The fluorescence kinetics of the model compounds measured at the magic angle is always singly exponential and independent of the emission wavelength.

The fluorescence kinetics of the oligomers and polymers (magic angle) show deviations from first-order decay and, in some cases, a dependence on the wavelength of the fluorescence detection. In these cases the mean fluorescence lifetime $<\tau>$ is calculated as $<\tau> = \sum a_i \tau_i / \sum a_i$, where a_i represents the amplitude of the *i*th decay component or, in the case of a time-resolved emission scan, the intensity in the steady-state fluorescence spectrum.

RESULTS AND DISCUSSION

Linear models and oligomers without alkoxy substitution

The absorption of the unsubstituted linear model compounds (**M1, M2, M3a**) is characterized by longest wavelength absorption maxima in the region $\lambda_a = 320$–350 nm and molar absorptivities $\varepsilon > 40000\ \mathrm{l\ mol^{-1}\ cm^{-1}}$ [Table 2(a)].

The bathochromic shift of the spectra increases with

Table 3. Rate constants of fluorescence, determined by Φ_f/τ and by the Strickler/Berg equation [k_f(SB)] and rate constants [$k_{nr} = (1 - \Phi_f)/\tau$] of radiationless deactivation

(a)

Code	R	Φ_f/τ (ns^{-1})	k_f (SB)[b] (ns^{-1})	k_{nr} (ns^{-1})
BPB[a]	—	1.2	1.0	0.31
M1	—	1.2	0.83	0.25
M2	—	1.4	0.91	0.07
M3a	—	1.4	0.89	0.44
M3b	OC_8H_{17}	0.82	0.52	0.05
M3c	$OC_{12}H_{25}$	0.74	0.50	0.09
M3d	$OC_{18}H_{37}$	0.89	0.52	<0.09
M4	—	>0.25	0.8[c]	>4.5
M5a	—	0.96	0.68	1.0
M5b	OC_8H_{17}	0.36	0.27	0.05
M6	$OC_{18}H_{37}$	0.41	0.34	0.05

(b)

Code	R	DP	$<\Phi_f/\tau>$ (ns^{-1})	k_f (SB)[b] (ns^{-1})	k_{nr} (ns^{-1})
LP1	H	≤4	1.6	—	1.0
LP2	OC_8H_{17}	10	0.89	0.26	0.54
LP3	OC_8H_{17}	13	1.0	0.38	0.51
LP4	$OC_{18}H_{37}$	6	0.78	0.34	0.64
LP5	$OC_{18}H_{37}$	11	0.64	0.46	0.69
LP6	$OC_{18}H_{37}$	19	0.82	0.45	1.0
AP1	H	≤4	1.1	0.49	1.3
AP2	$OC_{12}H_{25}$	19	0.63	0.24	0.48
AP4	$OC_{18}H_{37}$	25	0.53	0.27	0.32

[a] 1,4-bis-phenylethinyl-benzen.
[b] With ε from solvent chloroform.
[c] Measured in EtOH.

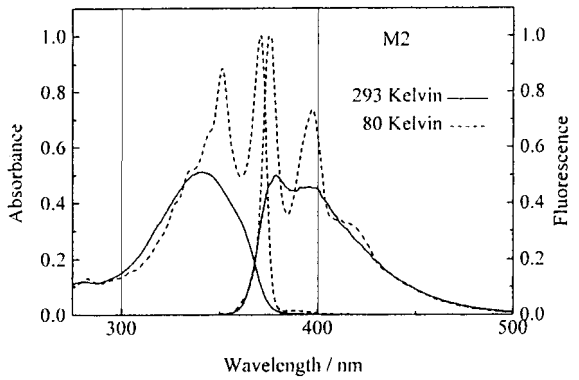

Figure 2. Absorption and fluorescence spectra of the model compound **M2** in EtOH at 293 and 80 K

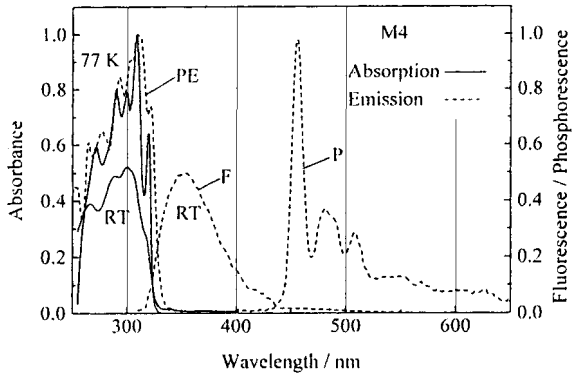

Figure 3. Spectra of the angular model compound **M4** in EtOH: absorption and fluorescence (F) spectra at room temperature and absorption, phosphorescence (P) and phosphorescence excitation (PE) spectra at 77 K

the number of the arylene units, i.e. with the extension of the aromatic system, as expected. The transitions are dipole allowed ($\pi\pi^*$) and polarized essentially parallel to the long molecular axis as revealed by semi-empirical calculations.

The fluorescence of these compounds is characterized by high quantum yields Φ_f and lifetimes τ less than 1 ns.

Figure 1 shows the absorption and the fluorescence spectra of the linear model compound **M3a** and of the short-chain (soluble) oligomer **LP1**, dissolved in toluene at room temperature. The coincidence of the absorption and the fluorescence excitation spectra of the model compounds **M1** and **M3a** is perfect and still satisfactory for the oligomer **LP1**.

The fluorescence spectra, especially of the models but to a lesser extent also with the oligomers, show a more pronounced vibrational structure than the absorption spectra. Such spectral behaviour is known for di- and higher aryleneethylenes and aryleneethinylenes. It is explained by the more rigid structure of the molecules in the S_1 state with respect to torsional motion around the formal single bonds. According to the Imamura–Hoffmann rules,[23] and also the NEER principle,[24] aromatic rings connected by a single bond become coplanar in the excited state with a considerably increased bond order. The deactivation rate constants at room temperature are given in Table 3. The fluorescence rate constants k_f calculated by the Strickler/Berg equation are smaller than the k_f value, calculated by Φ_f/τ in all cases. Obviously, the transition moments of the emission exceeds those of the absorption, and the molar absorptivity ε which is used in the Strickler/Berg equation for the description of the emission process gives too small an oscillator strength for the emission. This is in full accord with shallower torsional minima in the S_1 state. The same observation was made with distyrylstilbene and PPV derivatives.[25]

A decrease in temperature should lead to an increasing population of the lower torsional modes of the most stable S_0 and S_1 geometries. Consequently, the absorption spectra show a strong temperature dependence with the model compound **M2** in EtOH as an example (Fig. 2). While the structure of the fluorescence spectra at room temperature becomes clearer at low temperatures, the absorption spectra show a pronounced change. There is a bathochromic shift of the absorption maximum of 30 nm, and the structure shows mirror symmetry to the fluorescence. At low temperature the Stokes shift is very small, which indicates that the Franck–Condon states and the equilibrated states have essentially the same geometry in both the ground and the S_1 states.

The short-chain soluble linear unsubstituted oligomer **LP1** shows nearly the same absorption and fluorescence maxima as the corresponding model compound **M3a** (Fig. 1). Obviously, the relevant chromophore system of the unsubstituted oligomer is already realized in this model compound. We assume that the coplanar and perpendicular orientation of the rotating arylene units have nearly the same probability, which causes an effective segmentation. Rotation of the aromatic rings limits the number of coplanar rings to three as a statistical mean, thus preventing stronger long-wavelength absorp-

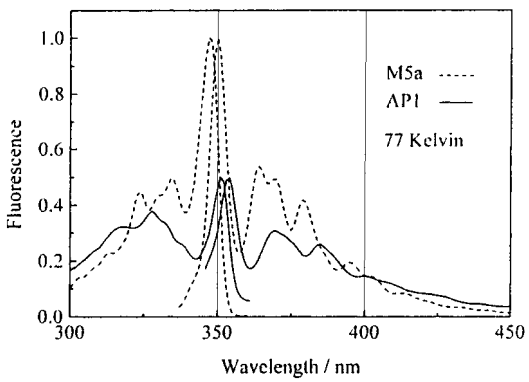

Figure 4. Fluorescence and fluorescence excitation spectra of the unsubstituted angular oligomer **AP1** (solid line) and the related model **M5a** (dashed line) in EtOH at 77 K

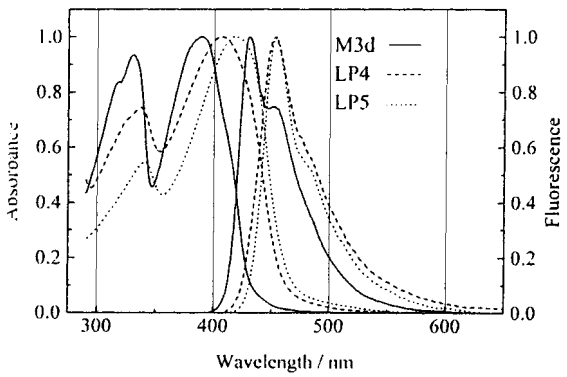

Figure 5. Absorption and fluorescence spectra of the substituted linear polymer **LP4** (dashed line), the linear oligomer **LP5** (dotted line) and the related model compound **M3d** (solid line) in toluene at room temperature

tion. Obviously, there is no geometrical relaxation in the S_1 state which would lead to a more extended and coplanar conjugated system because this should result in a significantly larger Stokes shift.

The oligomer shows a smaller fluorescence quantum yield and a shorter decay time in comparison with the model. Again, the rate constant of fluorescence, determined by Φ_f/τ (Table 3), is nearly the same as for **M3a**, supporting the assumption that **M3a** can be regarded as model for the oligomer. The enhanced radiationless deactivation can at least in part be due to intersystem crossing caused by the terminal bromine substituent. At 77 a weak phosphorescence was found.

Angular model compounds and oligomers without alkoxy substitution

The photophysical data of the angularly linked compound **M4**, the model **M1** and the angular oligomer **AP1** are also given in Table 2. A comparison of **M4** with the oligomers **AP1** reveals that **M4** cannot be regarded as model chromophore for **AP1**. **AP1** shows a remarkable bathochromic shift of both the absorption and the emission maxima and exhibits a higher fluorescence quantum yield and a longer decay time. The absorption of **M4** may be regarded as a superposition of two tolan units [tolan: $\lambda_a = 295$ nm, $\varepsilon = 29\ 000\ \mathrm{l\,mol^{-1}\,cm^{-1}}$, $\varepsilon(\mathbf{M4}) \approx 2 \times \varepsilon$ (tolan)]. Absorption and emission spectra of **M4**, recorded at room temperature and at 77 K, are shown in Fig. 3. While the fluorescence is still weak even at 77 K, an intense phosphorescence could be detected, indicating an efficient intersystem crossing deactivation channel of the S_1 state.

The fluorescence spectrum of **AP1** overlaps considerably with the absorption spectrum. It is not independent of the excitation wavelength. Similar effects were found for the substituted angular polymers and will be discussed below.

The fluorescence and the fluorescence excitation spectra of **AP1** and those of the model **M5a** in EtOH at 77 K are shown in Fig. 4. One may conclude from a comparison of the spectra that the linear model **M5a** is an appropriate model at least for the angular oligomer. This means that conjugation in the oligomer chain may be distorted mainly by torsion around the σ-bond connecting the pyridine rings of the bipyridyl moiety.

Semi-empirical calculations (INDO1/s after AM1 geometry optimization) of differently defined repetition units as a function of the number of repetition units are in full accord with **M1** and **M5a** being the most reasonable model compounds for the linear and angular polymers, respectively. Because of known shortcomings of these methods, and because a more detailed *ab initio* study is in progress (A. Göller and U.-W. Grummt, to be published), we will not go into details of these results. The absorption and emission spectra and the fluorescence rate constant, k_f, of the linear model **M1** closely resemble those of 1,4-bisphenylethinylbenzene (BPB) and **M5a** [cf. Table 3(a)]. Aza-substitution in the 4,4′-position of the aromatic rings of **M5a** merely leads to a faster radiationless deactivation process.

Alkoxy-substituted linear models, oligomers and polymers

Alkoxy substitution at the phenylene ring of the model compounds and polymers has a pronounced effect on the electronic structure of all compounds. The alkoxy substituents are electron donors which enhance the electron density in the ethinylene groups and hence increase the conjugation along the molecule.[2] This leads to a bathochromic shift of the longest wavelength absorption band of about 40 nm and a decrease of the absorptivity. The fluorescence spectra are concomitantly red shifted. An additional absorption band appears at ca 330 nm. Essentially the same effects of alkoxy substitution were found with PPV and distyrylbenzene derivatives.

Absorption and fluorescence data of three differently substituted linear models **M3b–d** are given in Table 2(a). The photophysical data and the spectra are essentially identical. They show that the length of the alkyl chain, at least for longer chains in solutions, has no influence on the photophysical properties in solution, as expected.

The absorption coefficient of the longest wavelength band is smaller in comparison with the unsubstituted model **M3a**. This indicates a smaller transition moment which also leads to the larger natural fluorescence lifetime $1/k_f$. Again the fluorescence quantum yield remains high. Thus, alkoxy substitution introduces no additional deactivation processes. The k_f values calculated from the spectra (according to the Strickler/Berg equation) and quantum yield and lifetime (Φ_f/τ) are given in Table 3(a).

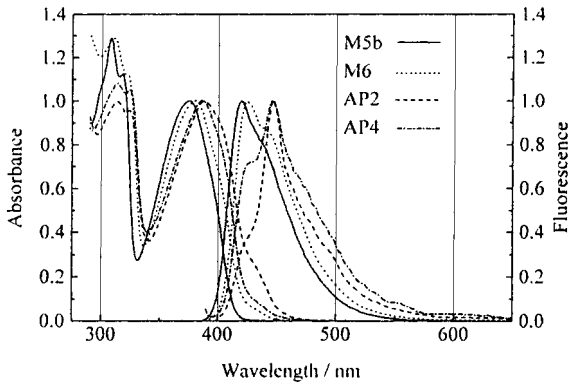

Figure 6. Absorption and fluorescence spectra of the substituted angular oligomer **AP2** (dashed line), angular polymer **AP4** (dash-dotted line) and related models **M5b** (solid line) and **M6** (dotted line) in toluene at room temperature

The relation between the values and their explanation are the same as in the case of unsubstituted models.

The absorption and the fluorescence spectra of the substituted linear model compound **M3d**, the linear substituted oligomer **LP4** and the polymer **LP5** are presented in Fig. 5. Evidently, there is a moderate bathochromic shift of the fluorescence between the model compound and the oligomer (DP ≈ 4). A larger degree of polymerization (DP = 20) leaves the emission wavelength nearly unchanged. The π-system is somewhat larger than that of the model compound **M3d**, by constrast with the unsubstituted **M3a** and **LP1**. Electron-donating alkoxy substituents increase the conjugation length. A second effect is the weakening of the 330 nm transition relative to the long wavelength absorption with increasing degree of polymerization.

The fluorescence spectra of the oligomers and polymers exhibit smaller bandwidths at room temperature than the absorption spectra, but they are essentially unstructured. In general, the fluorescence excitation spectra coincide with the absorption spectra, thus the most common criterion of the purity of fluorescent substances is fulfilled. Small differences do exist in the long-wavelength tail of the spectra. Frequently, the absorption spectra show a less steep edge and sometimes a long weak tail, which is absent in the excitation spectra. The origin of this tail is not yet clear. Usually, such findings indicate non-fluorescent impurities. With the bipyridyl-containing polymers various reaction side-products are conceivable,[26] some of which absorb at longer wavelengths: complexes with traces of metals, oxidation products, protonated bipyridyls and radicals. Metal complexes of bipyridylethinylenes have been described.[12] We measured the UV–visible spectra of new Ru complexes of models and polymers showing broad absorption bands in the region of 450 nm and emission quantum yields of the order of 10^{-2}.[27] Although all these side-products may also be formed with the model compounds, such long-wavelength tails are absent in the model compounds. Hence, the explanation by impurities or products is neither supported nor excluded. (Purification of the polymers from trace amounts of side-products is much more difficult! It cannot be excluded that traces of diethinylidene moieties are present in the polymer backbone owing to oxidative coupling during synthesis.) Further investigations to clarify this question are necessary.

The fluorescence quantum yields and lifetimes of the oligomers and polymers are reduced by ca 30% relative to the model compounds as a result of faster non-radiative deactivation of the polymers (cf. Tables 2 and 3). The fluorescence rate constants Φ_f/τ are essentially the same as those of the corresponding model compounds. The lower absorptivities of the polymers are at variance with this result because they should also lead to smaller Strickler/Berg radiative rate constants k_f(SB) (Table 3). The molar absorptivities are determined per unit weight of the repetition unit as usual. Probably, determination of the absorption coefficients per unit weight of the corresponding model compound would be more reasonable.

Alkoxy-substituted models and angular polymers

Figure 6 shows the absorption and fluorescence spectra of the angular polymers **AP2** and **AP4** and of the corresponding model compounds **M5b** and **M6**.

The spectra of these model compounds are not very different from those of the linear model compound **M3d**. They show the essential spectral features of the angular polymers. In comparison with the linear polymers, increasing chain length affects the spectra in a different way. The absorption spectra of the angular polymers are less red shifted with respect to those of their models and the short-wavelength transition retains the same intensity as the long-wavelength band. Both effects hint at a more effective hindrance of the π-conjugation in the angular polymers because of non-planar geometries present already in the σ skeleton due to rotations around the pyridyl–pyridyl single bond. This should also be the reason for the unusual fluorescence behaviour of the angular oligomers and polymers. The fluorescence and fluorescence excitation spectra depend on the excitation and emission wavelengths, respectively. This becomes more evident at lower temperature. The angular polymers should be better described as a multi-chromophore system rather than a molecule showing multiple fluorescence. In the case of segmented polymers with considerable conformational freedom, the existence of different absorbing and emitting units is readily conceivable. Especially the angularly linked polymers may exist in a large manifold of conformers by contrast with their linear counterparts which might be a tentative explanation. In particular, helical structures may be formed which might give rise to $\pi\pi$-stacking interaction in sandwiched chromophors.[28] However, this interpretation has to be

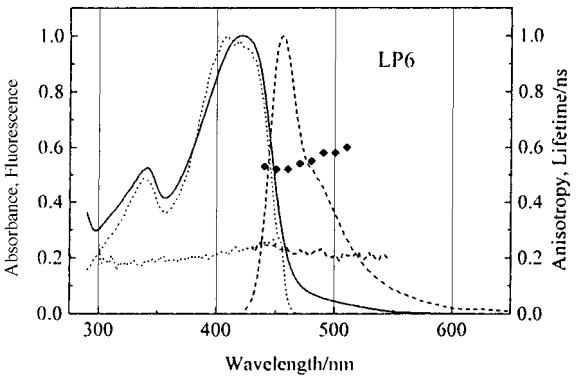

Figure 7. Absorption (solid line), fluorescence (dashed line) and fluorescence excitation (dotted line) spectra, excitation (dotted line) and emission (dashed line) anisotropy spectra (solid, dashed lines) and fluorescence lifetime (diamonds) of the linear polymer **LP6** in toluene at room temperature

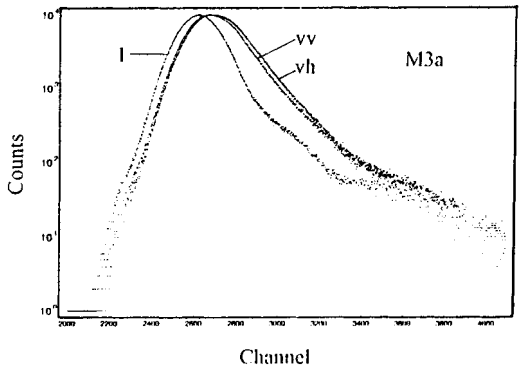

Figure 8. The vv and vh traces of the fluorescence kinetics of **M3a** in toluene at room temperature together with the excitation pulse profile (I); channel width = 6 ps

supported by further investigations. From the comparison of the low-temperature spectra, we conclude that **M5b** represents one subchromophore unit of the angular polymers.

Fluorescence kinetics

Fluorescence kinetics of the model compounds and the polymers were measured at room temperature using the polarizer and analyzer of the instrument. The fluorescence kinetics of the model compounds measured at the magic angle are always singly exponential and independent of the emission wavelength. The fluorescence kinetics of the oligomers and polymers (magic angle) show deviations from the first-order decay and depend in some cases a on the wavelength of the fluorescence detection. An example (**LP6**) is given in Fig. 7. The emission decay of the angular **LP2**, for instance, can be

Table 4. Lifetimes (τ), rotational relaxation times (ρ) and emission anisotropies (r) of polymers and model compounds in toluene and paraffin at room temperature

Code	DP a[a]	Solvent	τ (ns)	ρ_{calc}[b] (ns)	ρ_{exp}[c] (ns)	r_{calc}[d]	r_{calc}[e]	r_{exp}[f]
LP1	≤4	Toluene	0.38	≤1.62		≤0.276		0.17
	34.6	Paraffin	0.37	≤238		≤0.339		0.32–0.29
LP5	11	Toluene	0.75	12.3		0.320		0.27–0.23
	130	Paraffin	0.62/0.95	1800		0.340		0.33–0.30
LP6	19	Toluene	0.55	36.6		0.335		0.23–0.20
	164							
AP1	≤4	Toluene	0.42	≤2.45		0.290		0.16
	32.2	Paraffin	0.44	≤360		0.340		0.34–0.18
AP3	10	Toluene	0.72	15.3		0.325		0.15
	64.4	Paraffin		2250		0.340		0.30
AP2	19	Toluene	0.9	55.3		0.335		0.16
	153	Paraffin	0.65/1.35	8110		0.340		0.27
AP4	25	Toluene	1.18	96		0.336		0.15–0.12
	201							
M2	—	Toluene	0.69	0.17	0.17	0.068	0.067	0.068
	11.3	Paraffin	0.65	25		0.332		0.325
M3a	—	Toluene	0.55	0.25	0.26	0.106	0.11	0.13
	13.6							
M3b	—	Toluene	1.15	0.25	0.26	0.061	0.063	0.087
	13.6							
M3d	—	Toluene	1.12	0.25	0.34	0.063	0.079	0.09
	13.6	Paraffin	1.11	37		0.33		0.33

[a] Long molecular half-axis in Å (second values).
[b] Calculated by $\rho_{calc} = 4\eta\pi a^2 b/3kT$, η(toluene) = 0.6cP, η(paraffin) = 88cP, b = short half-axis.
[c] Calculated from polarized kinetic measurements.
[d] Calculated by $r_{calc} = 0.34/(1 + \tau/\rho_{calc})$.
[e] Calculated by $r_{calc} = 0.34/(1 + \tau/\rho_{exp})$.
[f] Calculated by $r_{exp} = (I_{vv} - GI_{vh})/(I_{vv} + 2GI_{vh})$ from steady-state fluorescence spectra.

described by two exponentials with 0.71 ± 0.08 and 1.46 ± 0.18 ns with relative yields of the faster component increasing smoothly from 62 to 83% in the wavelength region from 350 to 420 nm.

Emission anisotropy

The emission anisotropy gives valuable information about the directions of the transition moment of absorption and emission, rotational relaxation of molecules and energy transfer among molecules. The steady-state fluorescence polarization of two heteroarylene ethinylene polymers has been reported.[29] We performed polarized steady-state measurements with all models and polymers in solvents of different viscosity at room temperature and also time-resolved anisotropy measurements with selected compounds. An example of experimental vv and vh traces is given in Fig. 8 together with the excitation pulse.

The fluorescence anisotropy of all compounds is non-zero even in the low-viscosity solvent toluene owing to the rod-like shape of the molecules with the orientation of the transition moments parallel to the the long axis and the short fluorescence lifetimes. Table 4 gives experimental (exp) and calculated (calc) rotational relaxation times and emission anisotropies of polymers and model compounds in toluene and paraffin oil. Rotational relaxation times were measured only for the model compounds in toluene. Rotational relaxation times ρ_{calc} were calculated using the Stokes–Einstein equation for all compounds. The effective rotational volumes were assumed to be represented by a rotational ellipsoid with the long axis equal to the length of the rod-like models or polymers. The diameter of the linear or angular bipyridyl unit in the aromatic plane was taken as the short axis because semi-empirical calculations predict the possibility of nearly free rotation around the acetylene–(hetero)arene single bonds. The molecular dimensions of the models and of the repetition units of the polymers were obtained from simple molecular mechanics calculations (MM3) neglecting the alkoxy substituents. To obtain the dimensions of the polymers the corresponding repetition units were multiplied by the degree of polymerization. The results are presented in Table 4.

It is obvious that the rotational relaxation time of the model compounds in toluene, calculated from the molecular dimensions with the Stokes–Einstein equation, are in very good agreement with those determined from the polarized fluorescence kinetics. From this we conclude that the simple geometric model is suitable for a reasonable description of the depolarization of rod-like molecules.

From the calculated rotational relaxation times and the experimental steady-state emission anisotropies of the model compounds in the high-viscosity solvent paraffin, we determined the limiting emission anisotropy $r_0 = r_{exp}(1 + \tau/\rho_{calc}) = 0.34 \pm 0.02$. Similar values have been found by us for substituted distyrylbenzenes and have also been reported for a number of prolate stilbenes[30] and phenyloxazoles.[31]

Reasons why the the limiting anisotropy may deviate from the theoretical value $r_0 = 0.4$ (fundamental anisotropy of the S_0–S_1 transition) have been discussed by Kawski.[32] One possibility is a different orientation of the absorption and emission transition moments in the molecule. We determined the angle α between the absorption and the emission transition moments as 18° according to the equation $\cos^2\alpha = (3r_0 - 1)/5$.[33] Although the stilbene and phenyloxazole derivatives investigated by Kawski and the arylene ethinylenes in this work have different structures (sp^2-and sp-hybridisized carbon atoms in the chain, respectively), they do show the same fundamental anisotropies. Possibly the arylene ethinylenes with the bipyridyl units in the chain lose the linear structure of the ground state upon excitation to the S_1 state. Concerning the geometry of the excited subchromophores, contradictory results have been reported. For acetylene a transoid structure has been calculated for the S_1 state.[34] Hirata *et al.*[35] have presented strong experimental evidence in favour of a linear and coplanar diphenylacetylene in the first excited state (see also Ref. 36).

The other subchromophore 2,2′-bipyridine becomes asymmetric in the S_1 state according to time-resolved Raman experiments and *ab initio* calculations.[37] Detailed quantum chemical calculations for our systems are in progress (A. Göller and U.-W. Grummt, to be published).

For all model compounds in toluene and paraffin the emission anisotropies calculated from the Perrin equation with $r_0 = 0.34$ and with the different rotational times agree well with the values from steady-state measurements. In the case of the **oligomers and polymers**, the situation is more complicated: the measured emission anisotropies are mostly smaller than the calculated values and they are not constant over the fluorescence spectrum (see Fig. 7).

One reason for the smaller anisotropies could be the inadequate determination of the rotational volumes, especially of the alkoxy-substituted oligomers and of the cisoid angular polymers. Other reasons are depolarization mechanisms due to additional molecular motions which are not described by the simple rotational model used above and due to energy transfer processes. Energy transfer should take place in both the linear polymers and the angular polymers as calculated below (see Table 5). With rigid linear polymers intramolecular energy transfer along the chain alone should not alter the direction of the transition moment and hence should not diminish the emission anisotropy. However, energy transfer together with transversal or torsional vibrations might cause the smaller anisotropies observed in the low-viscosity solvent toluene. Torsional vibrations are assumed to be responsible for the devation of prolate molecules in low-

Table 5. (a) Data for Förster transfer along polymers in toluene and radiationless deactivation and (b) data for monomer 'donors' [cf. Table 2(a)] and 'acceptors' in toluene at room temperature

(a)

Polymer	Model	I_{DA}[a] (10^{-11} cm^6 mol^{-1})	κ^{2}[b]	R_0[c](Å)	r^{4d}(Å)	k_{et}[e](10^{11} s^{-1})	k_{nr}[f](10^9 s^{-1})
LP1	**M3a**	2.2	4	47.6	17.5	7.4	1.0
LP1	**M1**	2.2	4	48.2	17.5	6.5	1.0
LP6	**M3d**	4.6	4	56.3	17.5	9.9	1.0
AP1	**M5a**	2.4	3.24 (t)	43.3	15.5	9.4	1.3
			0.0625 (c)	22.4	10.5	1.9	
AP2	**M5b**	1.0	3.24 (t)		15.5	1.4	0.48
			0.0625 (c)		10.5	3.0	
AP4	**M5b**	0.69	3.24 (t)	38.7	15.5	1.0	0.32
			0.0625 (c)	29.4	10.5	2.0	

(b)

Model compound	R	$\Phi_{f,D}$	τ_D (ns)	ε_A[g] (l mol^{-1} cm^{-1})
M1	—	0.83	0.67	48900
M3a	—	0.76	0.55	49400
M3d	$OC_{18}H_{37}$	1	1.12	48000
M5a	—	0.49	0.51	40500
M5b	OC_8H_{17}	0.87	2.39	25000

[a] $I_{DA} = [\int F_D(\lambda)\varepsilon_A(\lambda)\lambda^2 d\lambda]/[\int F_D(\lambda)/\lambda^2 d\lambda]$ with absorption spectrum $\varepsilon_A(\lambda)$ and fluorescence spectrum $F_D(\lambda)$ from the polymers.
[b] $\kappa^2 = (\cos\Phi_{DA} - 3\cos\Phi_{DR}\cos\Phi_{AR})^2$; (t) transoid conformation, (c) cisoid conformation.
[c] $R_0^6 = 8.8\times10^{-28}\kappa^2\Phi_{f,D}/n^4 I_{DA}$.
[d] Estimated from model calculations (MM3).
[e] $k_{et} = 1/\tau_D(R_0/r)^6$; energy transfer in one direction.
[f] Data from Table 3.
[g] From chloroform as a solvent.

viscosity solvents from the Perrin equation, resulting in smaller rotational relaxation times. In highly viscous solvents the prolate molecules behave according to the Perrin equation.[38] Thus, in the high-viscosity paraffin oil the torsional vibrations are suppressed and the theoretical anisotropy approaches the experimental value.

A different situation is met with the angular polymers, which may exist in various geometries. In the limiting case of all-transoid geometry of the bipyridine moieties the transition moments of the chromophores in the chain are parallel to each other and the long molecular axis is large, resulting in high rotational relaxation times and high anisotropies. This case seems to be approximately realized in paraffin oil. The long aliphatic chains of the high viscous paraffin possibly promote all-transoid structures of the polymers.

In the limiting case of all-cisoid geometries, the transition moments of the chromophores in the chain are randomly oriented and the rotational relaxation time of the globular polymer is not so large. As a consequence, both molecular rotation and energy transfer should contribute to the depolarization of the fluorescence. This case seems to be realized to a larger extent in the low-viscosity solvent toluene.

The decrease of the anisotropy with the emission wavelength is primarily observed with the linear polymers. With all model compounds no emission wavelength dependence of the fluorescence anisotropy is observed, as expected for one-component systems. However, the polymers are characterized by a distribution of the chain length. In contrast to the models, the fluorescence kinetics are not singly exponential and vary within the fluorescence spectrum. From the observed increase in the mean decay times with the emission wavelength, a decrease in the emission anisotropy has to be expected. However, this effect alone cannot explain the measured values.

Hennecke *et al.*[39] reported a decrease in the anisotropy with the emission wavelength for poly(*p*-phenylenevinylene) in a polystyrene film, which they explained by the existence of various emitting species characterized by different lengths of excited segments. We observed this effect in diluted liquid solution where energy transfer along the polymer chain is much more probable than intermolecular transfer between different chains. The emission wavelength dependence should be also a consequence of this energy transfer. The larger the number of energy transfer steps becomes between absorption and emission of a photon, the larger should be the depolarization. From energetic reasons the most probable number of energy transfer steps should be larger for red than for blue photons, and hence the anisotropy becomes lower at the long wavelength tail of the fluorescence spectrum.

Energy transfer

Energy migration along phenyleneethinylene polymer chains and transfer to incorporated acceptors were investigated by fluorescence quenching experiments by Swager *et al.*[8] The same group investigated two polymers with related poly(phenyleneethinylene) structures,[9] and the all-*para* system was found to exhibit more efficient energy migration than the more electronically localized analogue which contains *meta* linkages. Energy migration along rigid-rod polymer chains has also been discussed by Liu.[4] It was described by an energy hopping model with a rate derived from the dipole–dipole energy transfer mechanism.

The rates of energy transfer from the initially excited segment to the first neighbouring segment in our polymers estimated by the Förster equation for some oligomers and polymers are given in Table 5.

The overlap integral was calculated using the shapes of the absorption and fluorescence spectra of the polymers; however, the more realistic molar absorptivities of the corresponding models were used instead of those of the polymers. Donor quantum yields and lifetimes were also taken from the corresponding model compounds, which were regarded as the donor parts in the polymer without energy transfer deactivation. Whereas the values of the overlap integrals are of the same order of magnitude for the different polymers, the parameter κ^2 depends strongly on the mutual orientation of the donor and acceptor transition moments.

In the linear polymers the maximum value $\kappa^2 = 4$ is assumed (neglecting the result of an angle of 18°). For the angular polymers only the two limiting cases of a transoid and a cisoid conformation of the donor–acceptor pairs in the same plane were investigated. Interestingly, the small κ^2 values of the cisoid conformations are compensated by shorter distances between donor and acceptor, which results in comparable energy transfer constants k_{et} of transoid and cisoid conformations. Generally, the rates of energy transfer are two to three orders of magnitude higher than the fluorescence rate constants, and many energy transfer steps can procede before a photon is emitted. A comparison with the rate constant of radiationless deactivation k_{nr} shows a correlation with k_{et}. A high k_{et} increases the probability of reaching a trap in the polymer chain which leads to radiationless deactivation.

CONCLUSIONS

Alternating linear rigid-rod and angular oligomers and polymers consisting of 2,2′-bipyridine and diethinylenebenzene units, although fully conjugated according to their structural formulae, are segmented to π-systems which comprise three (hetero)aromatic rings and two ethinylene units. Their spectroscopic and photophysical behaviour can be reasonably described by the model compounds 1,4-bis(3′-pyridylethinyl)benzene and 1,4-bis(4′-pyridylethinyl)benzene, respectively, including their alkoxy-substituted analogues. Whereas the absorption maximum is still slightly bathochromically shifted with an increase in the mean degree of polymerization from 4 to 20, the fluorescence band remains essentially unchanged. Possibly the emissive excited state wavefunction is less delocalized than that of the ground state.

The model compounds exhibit fluorescence quantum yields close to unity and short fluorescence decay times of around 1 ns. Fluorescence anisotropy and rotational relaxation times are consistent with the Stokes–Einstein equation and the Perrin equation. The absorption and emission spectra of the polymers and their radiative rate constants determined by fluorescence quantum yield and lifetime and according to the Strickler/Berg equation show a conjugation length of one to two repetition units. The conjugation along the chain is stronger in linear than in angular polymers and stronger in alkoxy-substituted than in unsubstituted polymers. In angular polymers at least two different emitting segments were found.

The shortened mean lifetimes and the reduced fluorescence quantum yields of the oligomers/polymers indicate an additional radiationless deactivation channel which is attributed to energy migration along the chain. Rates of energy transfer calculated for linear and angular polymers correlate with rates of radiationless deactivation.

The experimental limiting emission anisotropy of the model compounds agrees well with that obtained from the Stokes–Einstein equation and the molecular dimension in low-viscosity solvents. Deviations are observed in high-viscosity solvents and with the polymers in all solvents. The emission anisotropy becomes wavelength dependent with the polymers.

As a result of model calculations, energy migration along the polymer chain occurs in both the linear and angular polymers. Evidently, this contributes to the decrease in the emission anisotropy. In the case of the linear polymers, additional effects are essential to explain the anisotropy reduction also with the linear polymers, e.g. geometry changes in the excited states and low-frequency bending vibrations which render the perpendicular exciton component weakly allowed even with the rigid linear polymers.

A picosecond time-resolved anisotropy study is in progress together with theoretical investigations in order to obtain a more detailed quantitative interpretation of the emission anisotropy.

Acknowledgements

This work was funded in part by the Deutsche Forschungsgemeinschaft via the ‘Sonderforschungsbereich 196, Physik und Chemie Optischer Schichten.’ U.-W.G. acknowledges financial support by the Fonds der Chemischen Industrie.

REFERENCES

1. Yamamoto T, Yamada W, Tagaki N, Kizu K, Maruyama T, Ooba N, Tomaru S, Kurihara T, Kaino T, Kubota K. *Macromolecules* 1994; **27**: 6620–6626.
2. Wautelet P, Moroni M, Oswald L, Le Moigne J, Pham A, Bigot J-Y, Luzzati S. *Macromolecules* 1996; **29**: 446–455.
3. Nalwa HS. In *Handbook of Organic Conductive Molecules and Polymers* vol. 4, Nalwa HS (ed.) Wiley: Chichester, 1997; 261–361.
4. Liu G. *Macromolecules* 1993; **26**: 5687–5692.
5. Schumm JS, Pearson DL, Tour JM. *Angew. Chem.* 1994; **106**: 1445–1448.
6. Kondo K, Okuda M, Fujitani T. *Macromolecules* 1993; **26**: 7382–7382.
7. Morgan J, Rumbles G, Crystall B, Smith TA, Bloor D. *Chem. Phys. Lett.* 1992; **196**: 455–461.
8. Swager TM, Gil CG, Wrighton MS. *J. Phys. Chem.* 1995; **99**: 4886–4893.
9. Zhou Q, Swager TM. *J. Am. Chem. Soc.* 1995; **117**: 12593–12602.
10. Bourdin E, Davey A, Blau W, Delysse S, Nunzi JM. *Chem. Phys. Lett.* 1997; **275**: 103–107.
11. Holzer W, Penzkofer A, Gong S-H, Davey AP, Blau WJ. *Opt. Quantum Electron* 1998; **29**: 713–724.
12. (a) Ley KD, Whittle CE, Bartberger MD, Schanze KS. *J. Am. Chem. Soc.* 1997; **119**: 3423–3424; (b) Ley KD, Schanze KS. *Coordi. Chem. Rev.* 1998; **171**: 287–307.
13. (a) Egbe DAM, Klemm E. *Macromol. Chem. Phys.* 1998; **199**: 2683–2688; (b) Egbe DAM, Heise B, Klemm E. *Des. Monomers Polym.* in press.
14. (a) Takahashi S, Kuroyama Y, Sonogashira K, Hagihara N. *Synthesis*, 1980; 627–630; (b) Austin WB, Bilow N, Kellegan WJ, Lau KSY. *J. Org. Chem.* 1981; **46**: 2280–2286; (c) Stevens EB, Tour MM. *Macromolecules* 1993; **26**: 2420–2427.
15. Weder C, Wrighton MS. *Macromolecules* 1996; **29**: 5157–5165.
16. Giesa R, Schulz RC. *Macromol. Chem.* 1990; **191**: 857–867.
17. Romero FM, Ziessel R. *Tetrahedron Lett.* 1995; **36**: 6471–6473.
18. (a) Case M. *J. Am. Chem. Soc.* 1958; **80**: 2745–2748; (b) Wenckert D, Woodward RB. *J. Org. Chem.* 1983; **48**: 283–289; (c) Kazuaki N, Seiji S. *Chem. Lett.* 1994; **7**: 1267–1270; (d) Simpson PJ, Vinciguerra A, Quagliano JV. *Inorg. Chem.* 1963; **2**: 282–286.
19. (a) Alan R, Roney RB, Sasse WHF, Wade KO. *J. Chem. Soc. B* 1967; 106–111; (b) Cook MJ, Lewis AP, McAuliffe GSG, Skarda V, Thomson AJ, Glasper JL, Robbins DJ. *J. Chem. Soc., Perkin Trans. 2* 1984; 1293–1301; (c) Polin J, Schmohle E, Balzani V. *Synthesis* 1998; **3**: 321–324.
20. El-Ghayoury A, Ziessel R. *Tetrahedron Lett.* 1997; **38**: 2471–2474.
21. (a) Lin JT, Sun S-S, Wu JJ, Lee L, Lin K-J, Huang YF. *Inorg. Chem.* 1995; **34**: 2323–2333; (b) Lin JT, Sun SS, Wu JJ, Liaw Y-C, Lin K-J. *Organomet. Chem.* 1996; **517**: 217–226; (c) Egbe DAM, Heise B, Klemm E. *Des. Monomers Polym.* in press.
22. Demas JN, Crosby GA. *J. Phys. Chem.* 1971; **75**: 9912–1024.
23. (a) Klessinger M, Michl J. *Lichtabsorption und Photochemie Organischer Moleküle*. VCH: Weinheim, 1989; 39; (b) Imamura A, Hoffmann R. *J. Am. Chem. Soc.* 1968; **90**: 5379.
24. Mazzucato U, Momicchioli F. *Chem. Rev.* 1991; **91**: 1679–1719.
25. Birckner E, Grummt U-W, Rost H, Hartmann A, Pfeiffer S, Tillmann H, Hörhold H-H. *J. Fluoresc.* 1998; **8**: 73–80.
26. Heitz W. *Angew. Makromol. Chem.* 1994; **223**: 135–145.
27. Pautzsch T, Rode C, Klemm E. *J. Prakt. Chem.* 1999; **341**: 548–551.
28. Bassani DM, Lehn J-M, Baum G, Fenske D. *Angew. Chem.* 1997; **109**: 1931–1933.
29. Holzer W, Penzkofer A, Gong S-H, Bradley DDC, Long X, Blau WJ. *Polymer* 1998; **39**: 3651–3656.
30. Kawski A, Kukielski J, Baluk P, Lenczewska M. *Z. Naturforsch., Teil A* 1980; **35**: 466–467.
31. Kawski A, Kukielski J, Kaminski J. *Z. Naturforsch., Teil A* 1979; **34**: 1066–1069.
32. Kawski A. *Criti. Rev. Anal. Chem.* 1993; **23**: 459–529.
33. Perrin F. *Acta Phys. Pol.* 1936; **5**: 335–347.
34. Winkelhofer G, Janoschek R, Fratev F, Schleyer Rv. *Croat. Chem. Acta* 1983; **56**: 509–524.
35. Hirata Y, Okada T, Nomoto T. In *Jablonski Centennial Conference on Luminescence and Photophysics, Book of Abstracts*. Torun, 1998; 234;
36. Gutmann M, Gudipati M, Schönzart P-F, Hohlneicher G. *J. Phys. Chem.* 1992; **96**: 2433–2442.
37. (a) Buntinx G, Nasrecki R, Poizat O. *J. Phys. Chem.* 1996; **100**: 19380. (b) DeWaele V, Didierjean C, Buntinx G, Poizat O. In *Jablonski Centennial Conference on Luminescence and Photophysics, Book of Abstracts*. Torun, 1998; 123–124.
38. Kawski A, Kaminski J, Kukielski J. *Z. Naturforsch., Teil A* 1979; **34**: 702–707.
39. Hennecke M, Damerau T, Müllen K. *Macromolecules* 1993; **26**: 3411–3418.